Optimized design and performance of a shared pump single clad 2 μm TDFA

Robert Tench, Clément Romano, Jean-Marc Delavaux

HAL Id: hal-01766661
https://hal.archives-ouvertes.fr/hal-01766661

Submitted on 13 Apr 2018

Optimized Design and Performance of a Shared Pump Single Clad 2 µm TDFA

Robert E. Tench [a], Clément Romano [a,b], and Jean-Marc Delavaux [a]

[a] Cybel LLC, 1195 Pennsylvania Avenue, Bethlehem, PA 18018 USA
[b] Institut Telecom/Telecom ParisTech, 46 Rue Barrault, 75634, Paris France
robert.tench@cybel-llc.com

Abstract

We report the design, experimental performance, and simulation of a single stage, co- and counter-pumped Tm-doped fiber amplifier (TDFA) in the 2 µm signal wavelength band with an optimized 1567 nm shared pump source. We investigate the dependence of output power, gain, and efficiency on pump coupling ratio and signal wavelength. Small signal gains of >50 dB, an output power of 2 W, and small signal noise figures of <3.5 dB are demonstrated. Simulations of TDFA performance agree well with the experimental data. We also discuss performance tradeoffs with respect to amplifier topology for this simple and efficient TDFA.

Keywords: Fiber Amplifier, Thulium, 2000 nm, Silica Fiber, Single Clad

1. Introduction

Simplicity and optimization of design are critical for the practical realization of wide bandwidth, high power single clad Thulium-doped fiber amplifiers (TDFAs) for 2 µm telecommunications applications. Recent TDFAs [1,2] have reported 2 µm band amplifiers with output power > 2W, gain > 55 dB, noise figure < 4 dB, and optical bandwidth greater than 120 nm. While these designs achieve high optical performance, they employ two or more optical stages and multiple pump sources. Therefore, it is desirable to investigate designs using one amplifier stage and one pump source. In this paper we report on the design, simulation, and experimental performance of a one-stage single clad TDFA using an L-band (1567 nm) shared fiber laser pump source, as a function of pump coupling ratio, active fiber length, pump power, and signal wavelength. Our one-stage TDFA data compare well with recently reported performance of multi-stage, multi-pump amplifiers [2]. In addition, the simplicity of the single clad pump shared design and its potential for cost reduction offer a broad selection of performance for different applications.

The paper is organized as follows: Section 2 presents our experimental setup, a single stage TDFA with variable coupling in the pump ratio between co-pumping and counter-pumping the active fiber. Section 3 covers the dependence of simulated amplifier performance on active fiber length, pump coupling ratio, slope efficiency, and signal wavelength. Section 4 compares measurement and simulation of the TDFA performance. Section 5 contrasts our simple TDFA design with performance of a two-stage, three-pump amplifier as reported previously in [2]. Finally, Section 6 discusses design parameter tradeoffs for different TDFA applications.

2. Experimental Setup for Shared Pump Amplifier

The optical design of our one-stage single pump TDFA is shown in Figure 1. A single frequency 2 µm DML source (Eblana Photonics) is coupled through attenuator A and into the active fiber F1. Pump light from a multi-watt fiber laser P1 at 1567 nm is split by coupler C1 with a variable coupling ratio k (%).The two pump signals
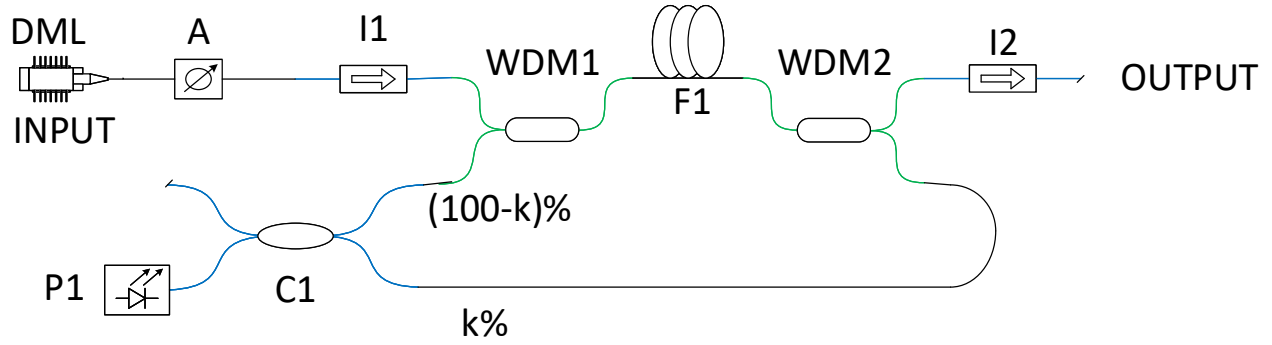
Figure 1. Optical Design of Single Stage Single Pump TDFA with a Shared Pump Arrangement.

WDM = Wavelength Division Multiplexer.

co-pump and counter-pump fiber F1, with k = 100% and k = 0% corresponding to all counter-pumping and all co-pumping, respectively. The value of k was changed in the simulations and experiments to optimize amplifier performance. Isolators I1 and I2 ensure unidirectional operation and suppress spurious lasing. Input and output signal powers, and co-pump and counter-pump powers, are respectively referenced to the input and output of Tm-doped fiber F1 (7 meters of OFS TmDF200). The input and output spectra of the TDFA were measured with an optical spectrum analyzer (Yokogawa AQ6375B).

3. Simulated Amplifier Performance

We begin the design of a high performance optical amplifier by studying the critically important variations of fiber signal gain (G) and output power (P_{out}) as a function of active fiber length (L) and input signal power (P_s).

The signal gain G is given by the following simple equation:

$$G(\lambda_s) = P_{out} (\lambda_s) / P_s (\lambda_s) \tag{1}$$

where λ_s is the signal wavelength, and P_s and P_{out} are signal powers measured at the input and output of the active Tm-doped fiber, respectively.

To study amplifier design we turn to the simulated TDFA performance [3,4] shown in Figure 2, where G is plotted vs. L for four input signal power levels. Here the total 1567 nm pump power (co- + counter-) (P_p) is 2.5 W, the signal wavelength λ_s is 1952 nm, and the coupling ratio k = 50%. We note that a similar set of gain curves can be generated for different wavelength bands of the TDFA, and this behavior will be investigated later in the section.

In Figure 2 we have measured the dependence of G vs. L for a 32 dB input dynamic range in signal power. The different P_s values illustrate the amplifier operating from a linear/unsaturated regime (P_s = - 30 dBm) to a highly saturated regime (P_s = + 2 dBm). The equally important dependence of noise figure on these parameters will be dealt with later.

The first observation drawn from Figure 2 is that for low input signals (e.g. for P_s = -30 dBm) G is maximized for long fiber lengths of 12 meters or greater, while for saturating input powers (e.g. P_s = +2 dBm) G reaches a maximum value for lengths of about 2 meters. It is also clear that for small signal or unsaturated gain, most of the gain (i.e. more than 80%) is achieved in the first 5 meters of the fiber, while for saturated gain most of the

gain occurs within the first 1.5 meters. The second observation is that saturated gain varies only slightly with active fiber length for values greater than 3 meters, indicating that a wide range of fiber lengths can be chosen for design of a power booster amplifier. However, later we will see that the choice of the fiber length affects the useful amplifier bandwidth.
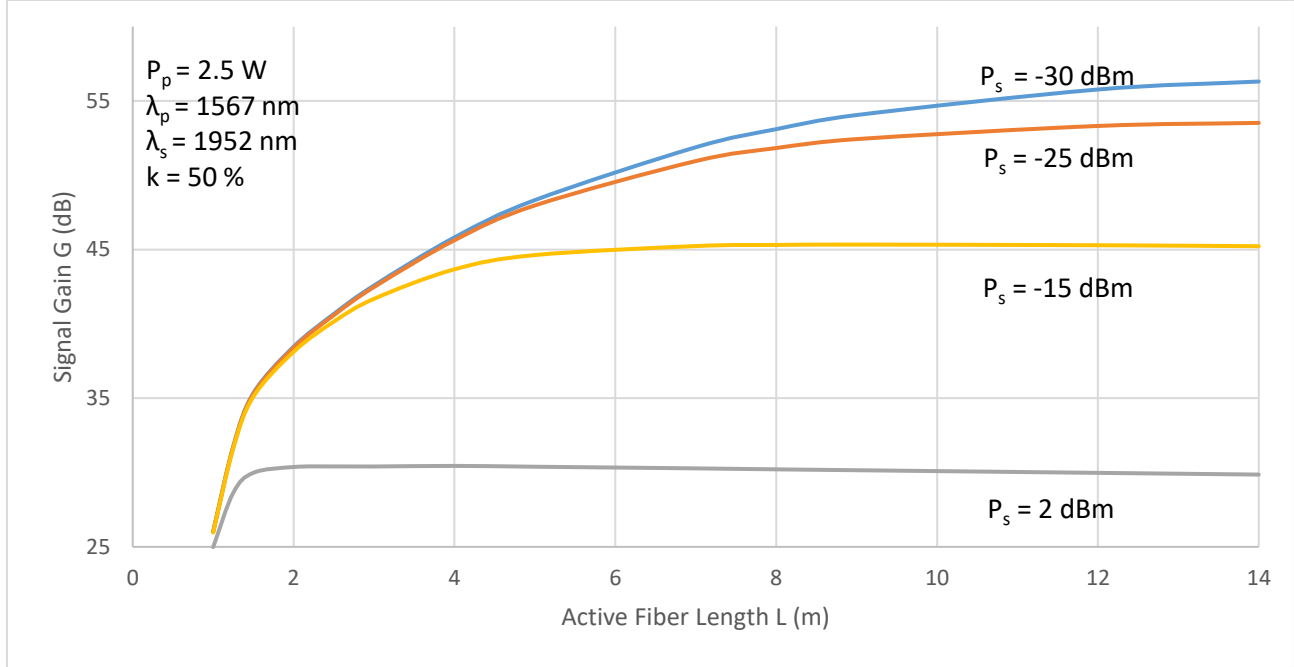

Figure 2. Signal Gain (G) as a Function of Fiber Length (L) for Four Different Levels of P_s.

The next design study for the shared pump amplifier is to examine the dependence of the saturated output power on active fiber length L and coupling ratio k. To study this issue, we plot the output signal power with pump coupling ratio k for four active fiber lengths (i.e. L = 3, 5, 7 and 9 m) as shown in Figure 3. In this simulation P_s is set to +2 dBm at 1952 nm to saturate the amplifier, with the total pump set at P_p = 2.5 W at 1567 nm.

We first note that for a given fiber length, P_{out} increases linearly when moving from co-pumping (k = 0%) to nearly all counter-pumping (k = 95%) and then drops down for full counter-pumping (k = 100%). For all fiber lengths, the maximum output power is achieved for k = 95%. This behavior is not surprising because counter-pumping maximizes the pump power available at the output of the fiber where the amplified signal power is the largest. We next observe that the maximum output power is achieved for a ratio of 95% counter-pumping to 5% co-pumping. For full counter-pumping, the pump is attenuated significantly within two meters after being launched, leaving the input end of the active fiber unpumped with no inversion achieved for the input Tm ion population. This indicates that a small amount of co-pumping provides signal gain that offsets fiber absorption loss. Therefore full counter-pumping is not the most efficient way to pump this amplifier.

For k = 50% in Figure 3, the relatively small variation in output signal power P_{out} with fiber length is consistent with the small variation in gain seen in Figure 2 as a function of fiber length for P_s = +2 dBm. We further note that as the fiber length is decreased from 9 m to 3 m, the output power P_{out} consistently increases. For very short fibers the difference between co-and counter-pumping will become negligible. However, as we will illustrate later, this comes at the expense of the amplifier operating bandwidth shifting from higher to shorter wavelengths.
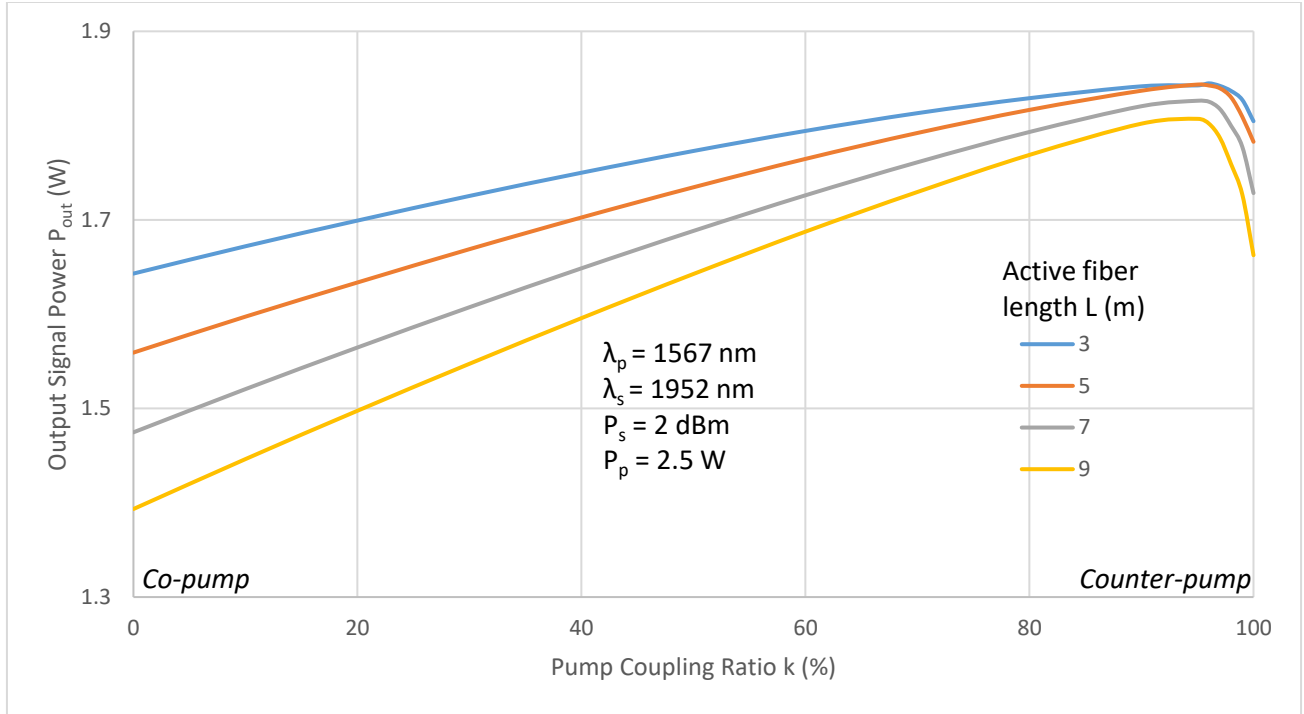
Figure 3. Simulated Output Signal Power (P_{out}) as a Function of Fiber Length (L) and Pump Coupling Ratio (k)

The amplifier performance illustrated in Figure 3 shows that we may consider three cases for design: k = 0%, k= 50%, and k = 95%. For k = 0%, P_{out} variation with fiber length is 18%. For k = 50%, it is as much as 10.9%, and for k = 95% it is about 2%. This indicates that a mostly counter-pumped amplifier will be less sensitive to changes in active fiber length than a co-pumped amplifier.

Now let's consider the important design consideration of the dependence of saturated output power as a function of active fiber length L and pump power P_p. This behavior is illustrated in Figure 4 for a signal wavelength of 1952 nm, a coupling ratio k = 50%, and 1567 nm pump powers of 0.83 W, 1.7 W and 2.55 W, respectively. In this plot we see that the maximum saturated output power is obtained for L = 2 m, relatively independent of fiber length and the pump power. It is apparent that above L = 2 m, P_{out} decreases slightly with increases in fiber length. This behavior is consistent with the simulation in Figure 2, and it illustrates that the optimum P_{out} for a saturated amplifier is not greatly dependent on L.
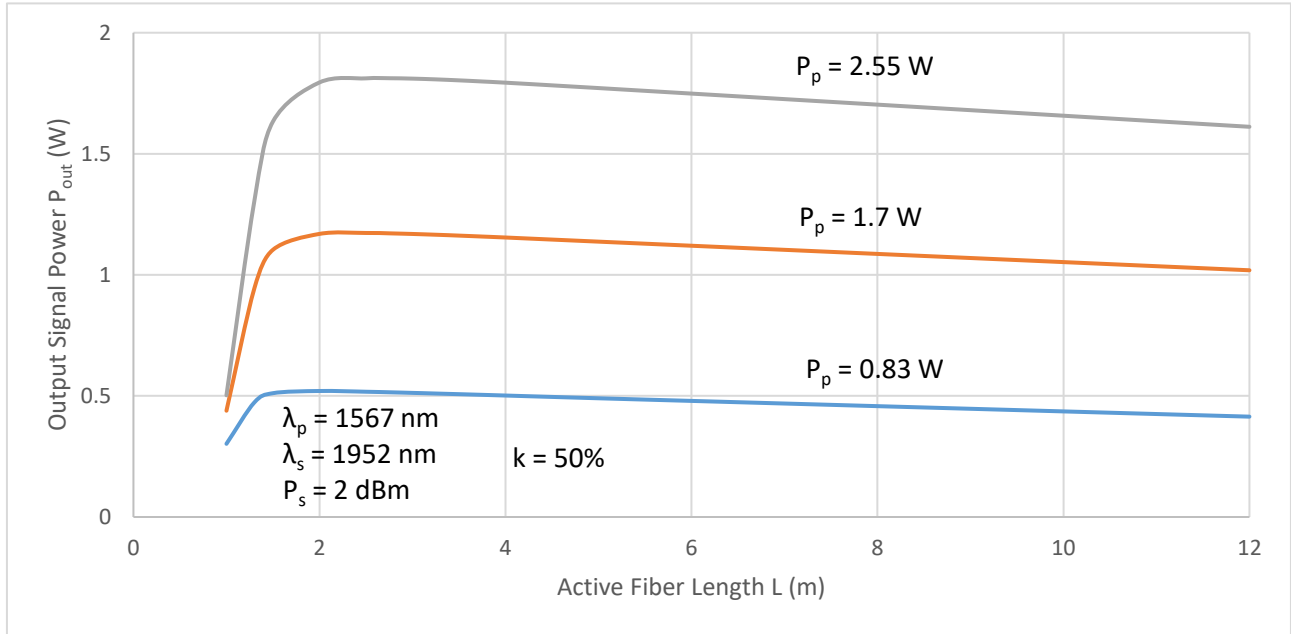
Figure 4. Simulated Output Power P_{out} as a Function of Fiber Length L and Pump Power P_p for k = 50%

The curves in Figure 4 lead to the important observation that the output power scales linearly with increases in the pump power. Therefore saturated output powers much higher than the 2.6 W already demonstrated [2] can be achieved with this type of Thulium-doped fiber up to the stimulated Brillouin scattering (SBS) threshold which is estimated to be 10-20 W for a fiber length of 7 m [9].

So far our simulations have been carried out for the signal wavelength of 1952 nm. To more fully study performance of the amplifier, we now look at the amplifier slope efficiency η vs. signal wavelength λ_s and active fiber length L. Slope efficiency $\eta = \Delta P_{sat}/\Delta P_p$ is defined as: the ratio of the change in saturated output signal power P_{sat} to a change in pump power, for a given fiber length L and signal wavelength λ_s. It measures the efficiency of conversion of pump light into signal light and is an important figure of merit for the amplifier. The saturated output power P_{sat} in our experiments and simulations is measured for a high input signal power P_s = +2 dBm.

Figure 5 shows simulations of η over the wavelength region of 1900 nm to 2050 nm, for fiber lengths ranging from 1.5 to 9 meters. Clearly the bandwidth of the amplifier shifts toward longer signal wavelengths for the longer fiber such as 9 meters. Shorter fibers such as 1.5 and 2 meters shift the operating bandwidth region toward shorter wavelengths.

Figure 5 indicates that for short fibers of 1.5 and 2 meters, η is optimum below 1950 nm, then diminishes rapidly with wavelength around 2000 nm and is negligible above 2020 nm. For longer fibers of 5 to 9 meters, η decreases more gradually with increasing wavelength and allows for a modest efficiency (i.e. 35%) up to 2050 nm. The simulated slope efficiencies in Figure 5 give a value at 1952 nm of 73% which is fully consistent with the value of 73% determined from Figure 4.
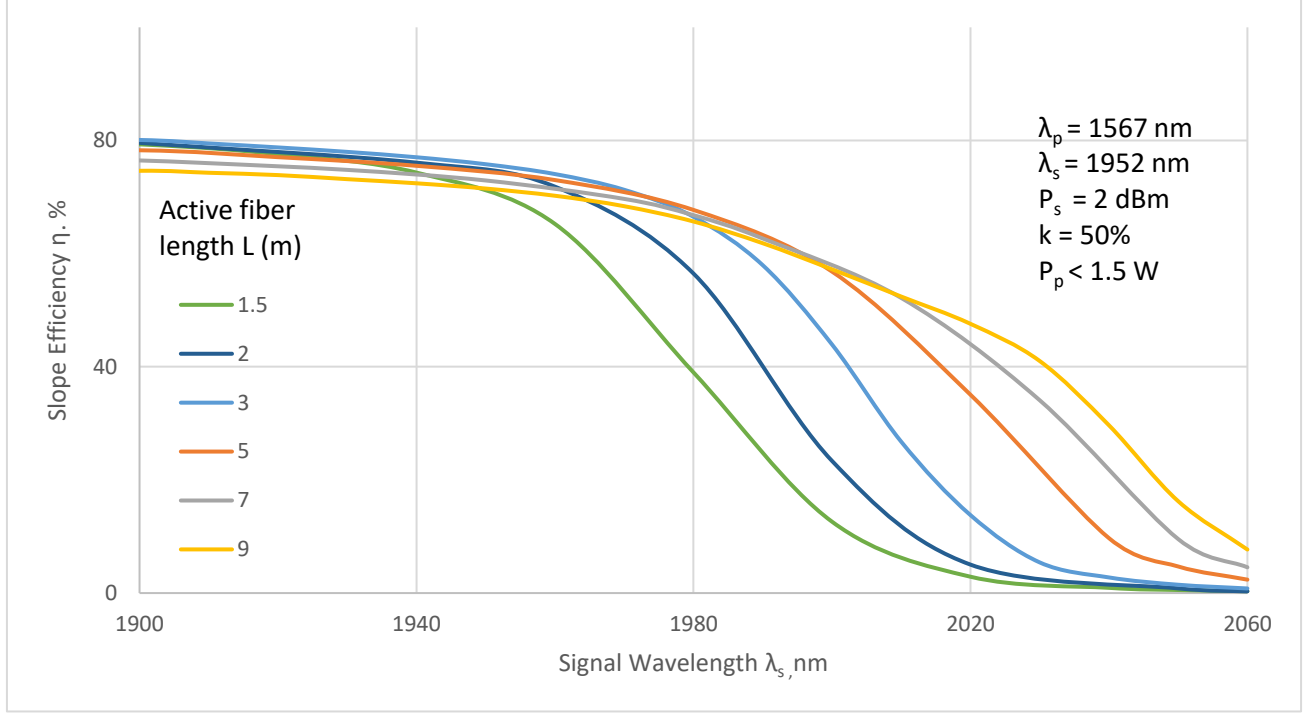
Figure 5. Simulated Slope Efficiencies η vs. Signal Wavelength λ_s and Active Fiber Length L

Based on the simulation results, for this single stage configuration we can draw four conclusions. First, the most significant gain occurs in the first couple of meters of the active fiber. Second, the saturated output power scales with pump power and is not significantly affected by the fiber length. Third, the optimum coupling ratio k for a combination of large dynamic range and saturated output power is achieved for medium fiber lengths of 6-8 meters and a k value around 50%. Fourth, the choice of the fiber length affects the operating bandwidth of the TDFA and the slope efficiency η: shorter lengths yield shorter operating wavelengths, while longer lengths give longer wavelength operating regions. This last point will be discussed further in Section 4.

4. Comparison of Simulation and Experiment

We now turn to comparisons of simulation and experiment for the single stage amplifier of Figure 1. In all these comparisons, the experimental fiber length is 7 meters.

We start by looking at the signal output power P_{out} as a function of 1952 nm signal input power P_s over a range of -30 dBm to + 2 dBm. Pump powers P_p at 1567 nm range from 0.89 W to 3.09 W and the coupling ratio k is 50%. As illustrated in Figure 6, the simulations (in solid lines) agree well with the experimental data (points) with an average difference between simulation and experiment of 0.6 dB.

For 0 dBm input power, the measured output powers are 1.11 W and 1.86 W for pump powers of 1.93 W and 3.09 W, respectively. This corresponds to optical power conversion efficiencies of 58% and 60%, respectively.
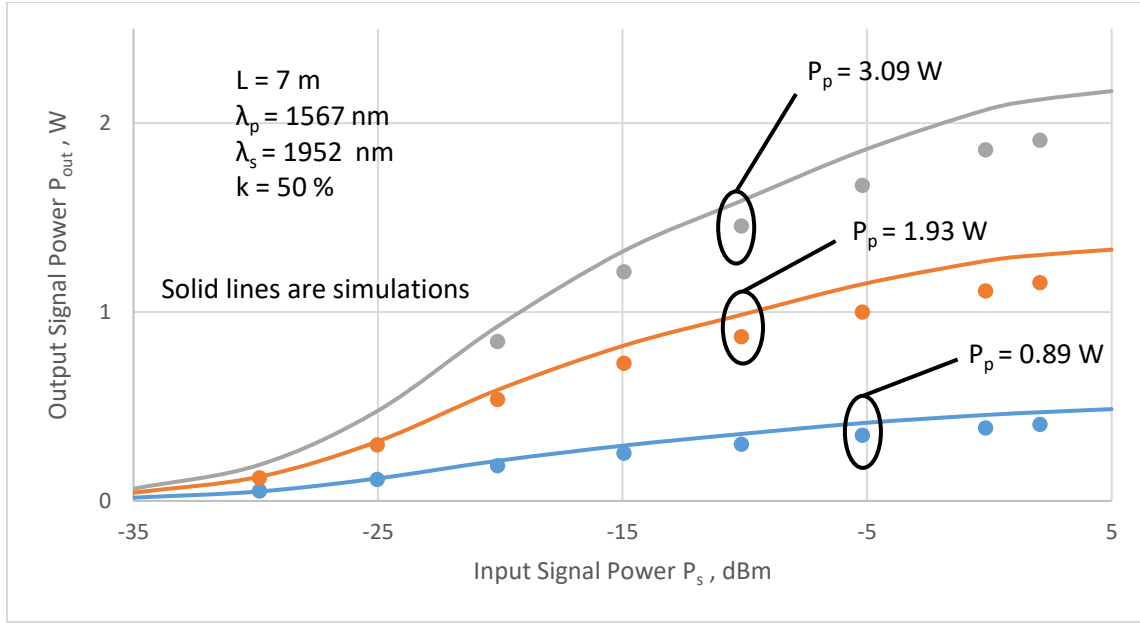
Figure 6. Output Signal Power P_{out} vs. Input Signal power P_s for k=50%, for Three Different Total Pump Powers P_p.

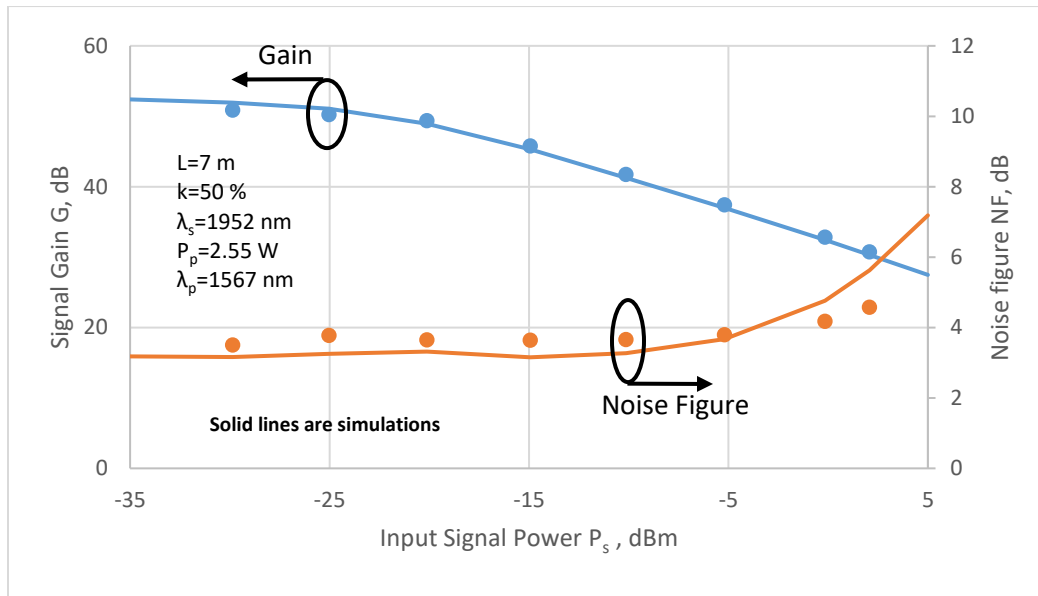Figure 7. Gain G and Noise Figure NF at 1952 nm as a Function of Input Signal Power P_s.

The next comparison of simulation and experiment is for small signal gain G and noise figure NF at 1952 nm as a function of signal input power P_s . For this comparison, we first need to define the noise figure NF. This is given by Equations (2) through (4) below (optical method of measuring noise figure) [10]:

$$N_{eq}(\lambda) = P_{ASE}(\text{forward}, \lambda_s) / (2\,h\,c^2\,\Delta\lambda / \lambda_s^{\,3})\,G(\lambda_s) \tag{2}$$

$$F(\lambda_s) = (1 / G(\lambda_s)) + 2\,N_{eq}(\lambda_s) \tag{3}$$

$$NF(\text{dB}) = 10\,\log_{10}(F(\lambda_s)) \tag{4}$$

In Equations (2) through (4), $\Delta\lambda$ is the effective resolution bandwidth of the optical spectrum analyzer in m, and P_{ASE} is the measured internal forward spontaneous output power under the signal peak in Watts. h is Planck's constant, and c is the speed of light in vacuum. $G(\lambda)$ is given by Equation (1). We measured the noise figure with a $\Delta\lambda$ of 0.1 nm on the Yokogawa optical spectrum analyzer.

Using Equations (1) through (4), we now analyze the performance of the TDFA as shown in Figure 7. A maximum signal gain G (points) of 51 dB is measured at $P_s = -30$ dBm with an NF < 3.5 dB. Over the full range of input powers studied, the simulated gain values (solid lines) agree with the measured gain values to within 1 dB, validating the performance of our simulator over a wide range of input powers. Experimental values of noise figure are also plotted in points in Figure 7. The minimum measured noise figure is 3.5 dB, and the minimum simulated noise figure is 3.2 dB, close to the 3.0 dB quantum limit. Agreement between experiment and simulation for noise figure is good. The measured dynamic range for the amplifier is 32 dB for a noise figure of 4.7 dB or less.

Figure 8 shows the dependence of G and NF on coupling ratio k for $P_s = -30$ dBm at 1952 nm and $P_p = 1.70$ W at 1567 nm. Experimental data are shown in points and the simulations in solid lines. The optimum operating setpoint for small signal gain is different from the optimum for noise figure, with the largest small signal gain occurring for k = 50% and the lowest noise figures for k = 0%. The noise figure increases slowly at first with k, and then rapidly to 6.1 dB as k reaches 100% which corresponds to counter-pump only. The agreement between simulation and experiment is good, validating the performance of our simulator over the full range of k values. From this graph, we observe that a good balance between optimum gain and optimum noise figure is achieved for a coupling ratio of k = 50%.
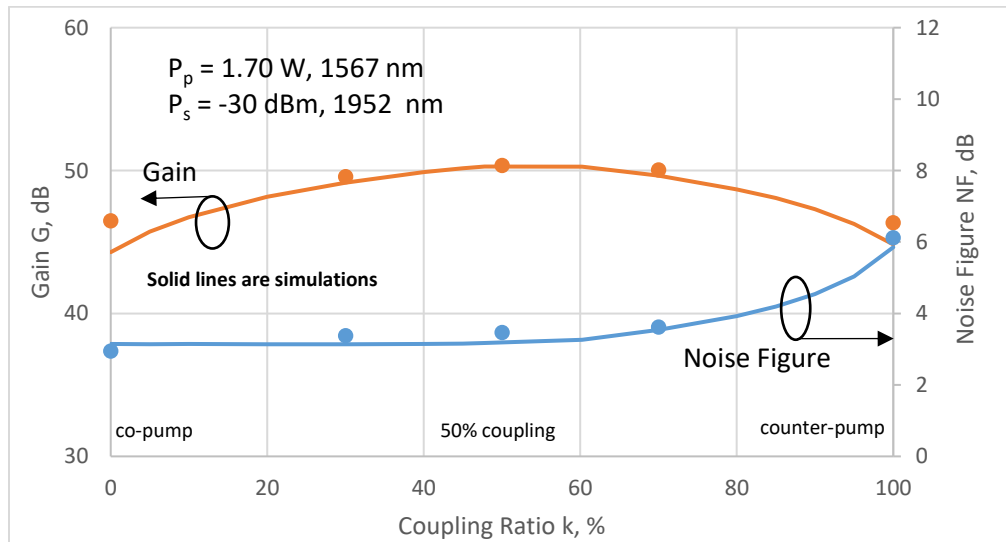

Figure 8. Gain and Noise Figure as a Function of Coupling Ratio k.

In Figure 9 we plot the dependence of G and NF on signal wavelength λ_s over the range of 1900 – 2050 nm for a coupling ratio of k = 50%, $P_p = 1.12$ W, and input signal power $P_s = -30$ dBm. The highest measured

unsaturated gain is achieved at 1910 nm , with a small decrease with λ at 1952 nm and then a steady decrease up to 2050 nm. For G > 30 dB, the amplifier bandwidth is >120 nm. By extending the investigation to values of λ lower than 1900 nm, we can expect even larger bandwidths.

The smallest measured NF of 3.5 dB is at 1952 nm, and NF variation with wavelength is small (i.e.< 1.4 dB). We observe that the agreement between simulation and experiment is good, and this shows our simulation predicts well the small signal gain G and noise figure NF as a function of λ_s.
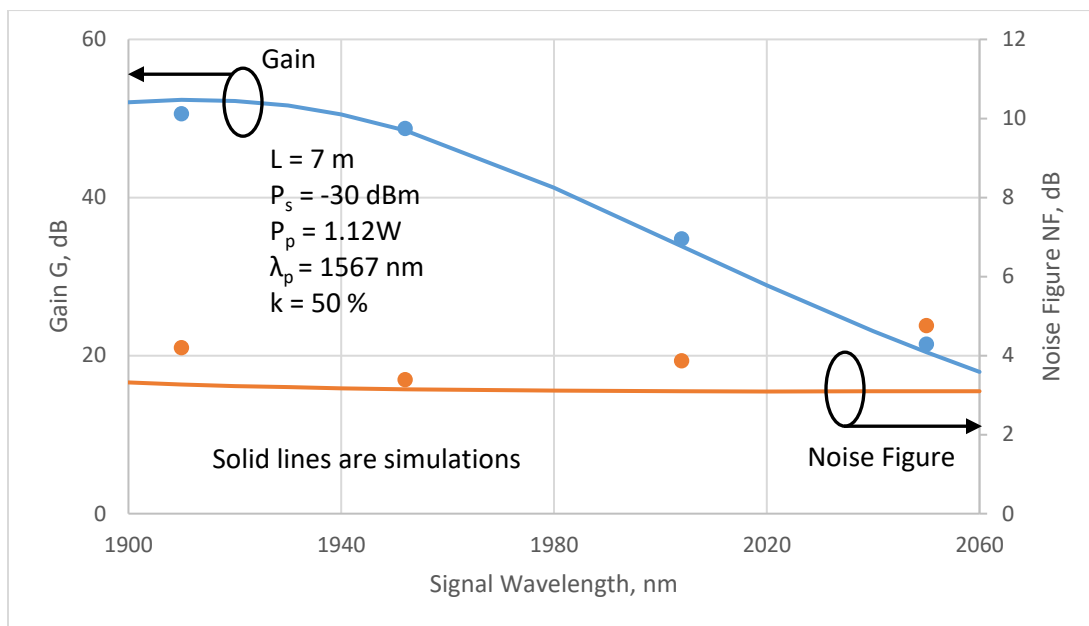

Figure 9 . Small Signal Gain G and Noise Figure NF as a Function of λ_s

We now investigate the slope efficiency η as a function of total pump power P_p for a saturating input power of $P_s \approx + 2$ dBm, Figure 10 shows experimental and simulated values for saturated output power as a function of pump power, for four different values of λ_s across the transmission band with k = 50%. The agreement between simulation (solid lines) and experiment (points) is good, illustrating the accuracy of our simulator over a wide region of λ_s and over pump powers from 0.3 to 3.2 W. Notice that at λ = 2050 nm the number of data points is limited by the onset of lasing due to the large ASE produced as the pump power increases. The experimental variation in signal output power with pump power is linear in all cases as expected from theory. The maximum measured output power is 2.00 W for λ = 1910 nm and pump power of 3.09 W, corresponding to an optical power conversion efficiency of 65%.
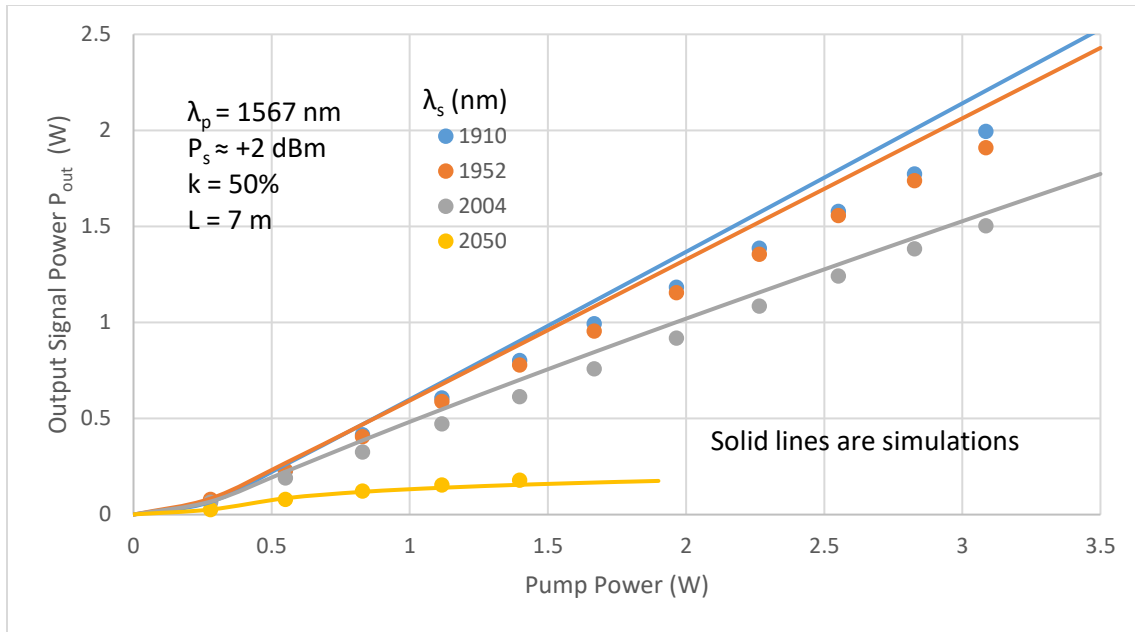
Figure 10. Saturated Output power P_{out} vs. Total Pump Power P_p as a Function of λ_s
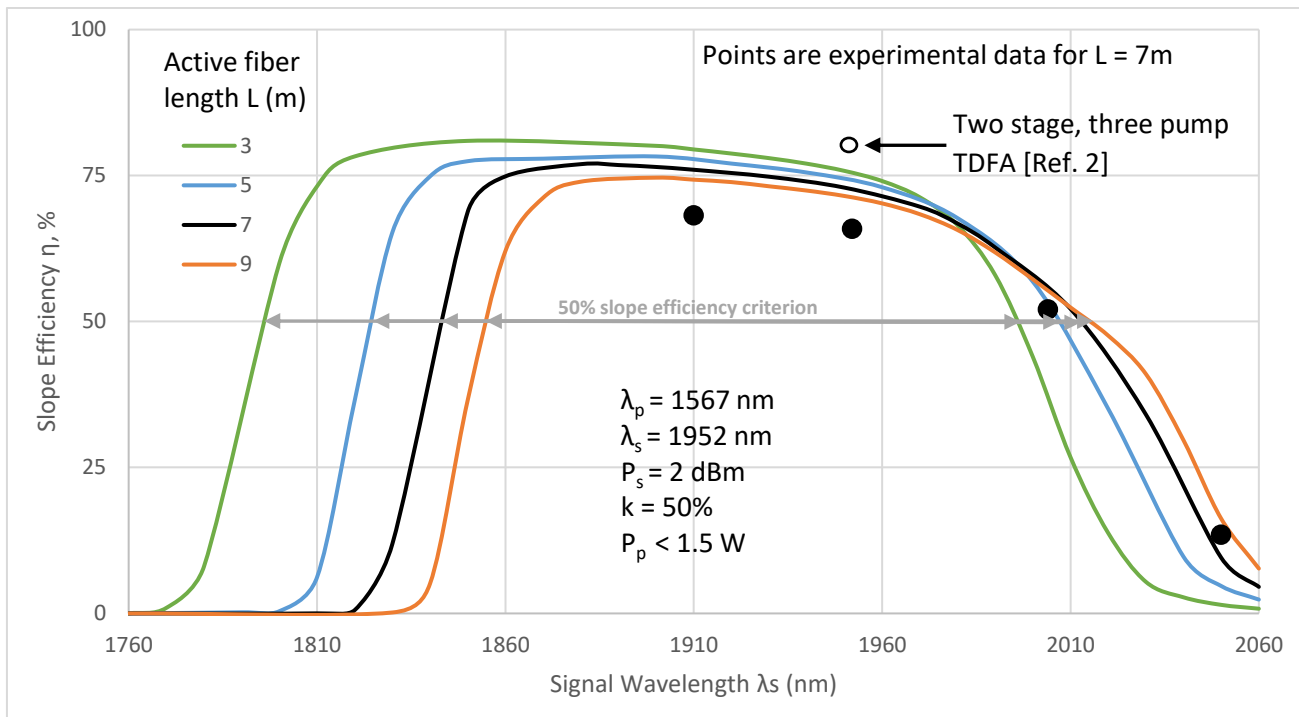

Figure 11. Simulated and Measured Slope Efficiency vs. λ_s as a Function of Fiber Length.

In Figure 11 we compare the slope efficiencies measured in Figure 10 with the simulation of Figure 5, with an expanded span for λ of 1760 nm – 2060 nm. The experimental slope efficiencies (points) agree reasonably well with the theory and this demonstrates that our simulation is valid over a wide range of values for λ_s for a saturated amplifier. The maximum measured slope efficiency is 68.2% at 1910 nm. This can be compared with the simulated value at this signal wavelength of 76.0%. Table 1 contrasts the measured and simulated values of slope efficiency η as a function of signal wavelength λ_s for a fiber length of 7 m.

λ, nm	η, %	
	Exp.	Sim.
1910	68.2	76.0
1952	65.9	72.9
2004	52.1	55.0
2050	13.5	9.6

Table 1 . Comparison of Simulated and Measured Slope Efficiency η as a Function of λ_s .

Using a slope efficiency of greater than 50% as a criterion, Figure 11 shows that the simulated operating bandwidth BW and center operating wavelength λ_c of the amplifier vary significantly with fiber length. For a short fiber (3 m) the operating bandwidth BW at 50% slope efficiency is 198 nm as indicated by the horizontal arrows in the figure, and λ_c is 1896 nm. For the longest fiber simulated (9 m) BW is reduced to 160 nm, and λ_c is shifted up in wavelength to 1940 nm. Results for all the fiber lengths

L, m	BW, nm	λ_c, nm
3	198	1896
5	182	1918
7	167	1932
9	160	1940

Table 2. Operating Bandwidth BW and Center Wavelength λ_c as a Function of Fiber Length L.

studied are summarized in Table 2. It is evident that shorter fiber lengths give greater operating bandwidths and lower center wavelengths. This behavior is consistent with previously reported results [6]. We note that Figure 11 and Table 2 are the first detailed comparisons of TDFA simulation and theory, since previous work on spectral performance has been either wholly experimental [5,6] or theoretical [7,8].

5. Comparison of Multistage Amplifier Performance

In Sections 3 and 4, we have shown that the shared pump topology can deliver high performance that is fully in agreement with simulation results. Here we will compare the shared pump amplifier with a two stage-three pump TDFA [2]. A summary comparison of the two amplifiers is given below in Table 3.

Fiber Length L = 7 m			TDFA Configurations, 1952 nm	
Parameter	Symbol	Units	1 Stage, Shared Pump	2 Stage, 3 Pumps
Pump Power (1567 nm)	P_p	W	3.2	3.6
Saturated Output Power	P_{out}	W	1.9	2.6
Small Signal Noise Figure	NF	dB	3.4	3.2
Signal Dynamic Range	P_{in}	dB	32	32
Small Signal Gain	G	dB	51	56
Slope Efficiency (Saturated)	η	%	65.9	82
Operating Bandwidth	BW	nm	167 (simulated)	> 120 (est. from ASE)

Table 3. Comparison of Single Stage, Shared Pump TDFA with Two Stage, Three Pump TDFA

The table reveals that there is no major difference in performance between the two TDFAs. Comparing the maximum saturated output powers, we see that the shared pump TDFA achieves 1.9 W output for 3.2 W available pump, while the 2 stage amplifier achieves 2.6 W for 3.6 W of available pump. The output power performance of the two amplifiers is seen to be comparable when the maximum pump power available is accounted for. NF values for the two amplifiers are similar, as are the operating dynamic ranges (measured over an input power span of -30 dBm to +2 dBm). The two-stage amplifier has a slightly higher small signal gain with 56 dB compared to 51 dB for the shared pump single stage TDFA.

The difference in slope efficiencies, with 66% for the 1 stage shared pump configuration and 82% for the 2 stage, 3 pump configuration, can be explained by referring to the architecture of the 3 pump configuration [2]. Here we recall the definition of slope efficiency η from Section 3: $\eta = \Delta P_{sat}/\Delta P_p$. Remembering that P_{sat} is the output power for a highly saturated amplifier, we observe that in the 2 stage TDFA the first stage boosts the input signal power of +2 dBm to an intermediate level of about +20 dBm which is then input to the second fiber stage. This boost in power to +20 dBm increases the conversion efficiency for available pump power in the second stage and so increases η. Indeed the two stage amplifier brings the measured efficiency closer to the simulated value as shown in Figure 11.

In comparing the amplifier bandwidth for the two configurations, we see that the 167 nm simulated bandwidth for the one stage, shared pump amplifier is consistent with the estimated value of >120 nm for the two stage, three pump amplifier. The >120 nm value was obtained by measuring the 10 dB width of the ASE noise background in the saturated output spectrum of the two stage TDFA. We believe that a simulation of the slope efficiency for the two stage amplifier (currently in progress) will result in a more precise value for its bandwidth.

The comparisons in Table 3 illustrate that our single stage shared pump TDFA can match the performance targets of a complex two stage three pump amplifier. The simplicity of the architecture of the shared pump TDFA is a considerable advantage in the design simulation of TDFAs for broadband telecommunications systems.

6. Discussion of Parameter Optimization for TDFA Architecture

The data reported in Figures 2 – 11 illustrate several salient points about the operation of the shared pump TDFA.

From our experimental and theoretical studies, it is evident that input power levels, saturated output power targets, noise figure specifications, small signal gain specifications, and operating signal bandwidths all depend in an interrelated way on the amplifier architecture. Design of an optimized amplifier requires a careful balancing of all these performance targets as a function of fiber length L and coupling ratio k.

For gain amplifiers, Figure 2 shows that it is very important to consider the input signal power when choosing an optimum fiber length. For example, at the coupling ratio of 50%, the fiber gain for – 30 dBm input is highest for a fiber length of 14 meters. For – 15 dBm input, the optimum gain occurs for lengths of 7-8 meters. Clearly the design specifications of the TDFA must be carefully considered when choosing an optimum fiber length for a preamplifier designed to operate at low signal input powers. For these low input powers the NF value remains close to the quantum limit of 3 dB.

For power amplifiers, maximum simulated output power occurs for a coupling ratio of k = 95% and an optimized fiber length of about 3.5 meters for a signal wavelength of 1952 nm. This optimized fiber length agrees well with the values obtained in Figures 2 and 4 where the optimum length for maximum output power is between 3 and 4 meters for a pump coupling ratio of 50 %. We conclude that for maximizing output power at 1952 nm, coupling ratios anywhere between 50 and 95 % can be employed.

Figure 4 demonstrates that the saturated output power P_{out} scales linearly with pump power up to the maximum simulated P_p of 2.55W. No Brillouin scattering or other nonlinear effects were observed in our experiments. This means that we can improve the output power of the amplifier simply by increasing the pump power, up to the limit where nonlinear effects start to be observed. The threshold for nonlinear effects in our shared pump amplifier is currently under study. For the parameters in the current experiments, the one stage shared pump design yields an attractive power amplifier that is simple to build and has high signal output power

For generic or multipurpose amplifiers, Figure 5 and 11 illustrate that the operating bandwidth BW and center wavelength λ_c of the amplifier are strongly dependent on the active fiber length, with maximum long wavelength response above 2000 nm occurring for fiber lengths L of 9 meters and longer. Short wavelength response is maximized for short fiber lengths of 1.5 and 2 meters. The desired operating bandwidth and center wavelength can therefore be selected by choosing an appropriate active fiber length. The noise figure NF as shown in Figure 9 is slowly varying with signal wavelength λ_s for a coupling ratio of k = 50 %, indicating that the noise performance of the multipurpose amplifier is highly tolerant of variations in signal wavelength λ_s. This is an attractive feature for the many applications of this type of TDFA.

To conclude, we have shown that an active fiber length L of 7 meters and a coupling ratio k = 50 % provide balanced performance over a wide range of operating parameters for the one stage, shared pump TDFA.

7. Summary

We have reported the experimental and simulated performance of a single stage TDFA with a shared in-band pump at 1567 nm. In particular we considered the dependence of amplifier performance on pump coupling ratio and signal wavelength. We determined that the optimum fiber length L and optimum coupling ratio k depend strongly on the design performance specifications for the TDFA such as signal wavelength band, saturated output power, noise figure, small signal gain, and dynamic range. Our simulations show that the operating bandwidth of the amplifier can be as high as 198 nm. Due to the broad Thulium emission bandwidth, this amplifier configuration can be tailored to meet a variety of performance needs. We achieved saturated output

powers of 2 W, small signal gains as high as 51 dB, noise figures as low as 3.5 dB, and a dynamic range of 32 dB for a noise figure of less than 4.7 dB. In all cases we found good agreement between our simulation tool and the experiments. No Brillouin scattering or other nonlinear effects were observed in any of our measurements. Our experiments and simulations show that the shared pump TDFA can match the performance of more complex multistage, multi-pump TDFAs, and illustrate the simplicity and usefulness of our design. This opens the possibility for new and efficient TDFAs for lightwave transmission systems as preamplifiers, as in-line amplifiers, and as power booster amplifiers.

8. Acknowledgments

9. References

[1]   C. Romano, R. E. Tench, Y. Jaouen, and G. Williams, "Simulation and design of a multistage 10 W thulium-doped double clad silica fiber amplifier at 2050 nm," in Proc. SPIE **10083**, Fiber Lasers XIV: Technology and Systems, 100830H (February 22, 2017).
[2]   R. E. Tench, C. Romano, and J.-M. Delavaux, "Broadband 2 W Output Power Tandem Thulium-doped Single Clad Fibre Amplifier for Optical Transmission at 2µm," Paper M.2.B.2, ECOC 2017, Gothenburg, Sweden.
[3]   C. Romano, R. E. Tench, Y. Jaouen, and J.-M. Delavaux, "Characterization of the 3F4 – 3H6 Transition in Thulium-doped Silica Fibres and Simulation of a 2µm Single Clad Amplifier," Paper P1.SC1.2, ECOC 2017, Gothenburg, Sweden.
[4]   S. D. Jackson and T. A. King, "Theoretical modeling of Tm-doped silica fiber lasers," J. Lightwave Technology **17**, no. 5, pp. 948–956, May 1999.
[5]   Z. Li, A. M. Heidt, N. Simakov, Y. Jung, J. M. O. Daniel, S. U. Ulam, and D. J. Richardson, "Diode-pumped wideband thulium-doped fiber amplifiers for optical communications in the 1800-2050 nm window," Optics Express **21**, 26450-26455 (2013).
[6]   Z. Li, Y. Jung, J.M.O. Daniel, N. Simakov, M. Tokurakawa, P. C. Shardlow, D. Jain, J. K. Sahu, A. M. Heidt, W. A. Clarkson, S. U. Ulam, and D. J. Richardson, "Exploiting the short wavelength gain of silica-based thulium-doped fiber amplifiers," Optics Letters **41**, 2197-2200 (2016).
[7]   M. Gorjan, T. North, and M. Rochette, "Model of the amplified spontaneous emission generation in thulium-doped silica fibers," J. Opt. Soc. Am. B, 2886-2890 (2012)
[8]   M. A. Khamis and K. Ennser, "Theoretical Model of a Thulium-doped Fiber Amplifier Pumped at 1570 nm and 793 nm in the Presence of Cross Relaxation," J. Lightwave Technology **34**, 5675–5681 (2016).
[9]   A. Sincore, N. Bodnar, J. Bradford, A. Abdulfattah, L. Shah, and M. C. Richardson, "SBS Threshold Dependence on Pulse Duration in a 2053 nm Single-Mode Fiber Amplifier," J. Lightwave Technology **35**, 4000-4003 (2017).
[10]   E. Desurvire, "Erbium-Doped Fiber Amplifiers: Principles and Applications", New York, Wiley Interscience (1994), Eqs. 5.32 and 5.34.